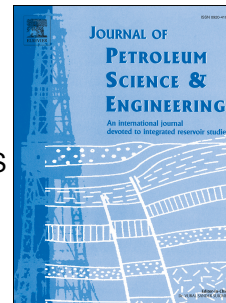


# Accepted Manuscript

Numerical model and program development of TWH salt cavern construction for UGS

Jifang Wan, Tianji Peng, Ruichen Shen, Maria Jose Jurado



PII: S0920-4105(19)30364-X

DOI: <https://doi.org/10.1016/j.petrol.2019.04.028>

Reference: PETROL 5967

To appear in: *Journal of Petroleum Science and Engineering*

Received Date: 2 January 2019

Revised Date: 30 March 2019

Accepted Date: 8 April 2019

Please cite this article as: Wan, J., Peng, T., Shen, R., Jurado, M.J., Numerical model and program development of TWH salt cavern construction for UGS, *Journal of Petroleum Science and Engineering* (2019), doi: <https://doi.org/10.1016/j.petrol.2019.04.028>.

This is a PDF file of an unedited manuscript that has been accepted for publication. As a service to our customers we are providing this early version of the manuscript. The manuscript will undergo copyediting, typesetting, and review of the resulting proof before it is published in its final form. Please note that during the production process errors may be discovered which could affect the content, and all legal disclaimers that apply to the journal pertain.

# Numerical Model and Program Development of TWH Salt Cavern Construction for UGS

Jifang Wan<sup>a,b</sup>, Tianji Peng<sup>c,\*</sup>, Ruichen Shen<sup>d</sup>, Maria Jose Jurado<sup>b</sup>

*a Research Institute of Petroleum Exploration and Development, Beijing 100083, China*

*b Institute of Earth Sciences Jaume Almera, CSIC, Barcelona 08028, Spain*

*c Institute of Modern Physics, Chinese Academy of Sciences, Lanzhou 730000, Gansu, China*

*d CNPC Engineering Technology R&D Company Limited, Beijing 100097, China*

## Abstract

Underground TWH caverns in salt rock have high construction efficiency and large usable volumes and provides an ideal space for large-scale natural gas storage. In this study, the solution mining process of TWH cavern is thoroughly analyzed. Applying basic principles of the Navier-Stokes equation method and reasonable assumptions, we established a new 3D mathematical model which includes flow and mass transfer and boundary movement for TWH salt cavern construction. Then, the velocity field and the concentration field can be solved by the SIMPLE algorithm, while the boundary movement of cavern expansion can be solved by the VOF algorithm. We developed a new VC++ computer code program TWHS MC for solution mining and herein we present the numerical results. Finally, the simulation cavern shapes results by program are compared with the experimental ones. The results indicate that our model successfully and accurately predicts the cavern shape and demonstrates the reliability and applicability of the model.

## Keywords:

Underground gas storage; Two-well-horizontal cavern; Numerical model; Program development; Cavern expansion

---

\*Corresponding author:

E-mail address: pengtianji@163.com.

Postal address: Institute of Modern Physics, Chinese Academy of Sciences, Lanzhou of Gansu Prov. 730000, P. R. China.

Tel.: +86 09314969914.

## 24 **Abbreviations**

25	UGS:	Underground gas storage
26	TWH:	Two-well-horizontal
27	TWV:	Two-well-vertical
28	SWV:	Single -well-vertical
29	2D:	Two dimensional
30	3D:	Three dimensional
31	SIMPLE:	Semi-Implicit Method for Pressure-Linked Equations
32	VOF:	Volume of Fluid
33	TWWSMC:	Two-well-horizontal Solution Mining Cavern
34	CFD:	Computational Fluid Dynamics
35	N-S:	Navier-Stokes
36		

## 37 1. Introduction

38 Because of its low permeability and good self-healing capacity, salt rock is recognized as an  
39 ideal medium for large-scale energy high capacity storage (Yang et al., 2015) such as strategic  
40 petroleum reserves (SPR) (Liu et al., 2016; Zhang et al., 2017), compressed air energy storage  
41 (CAES) (Aghahosseini and Breyer, 2018; Budny et al., 2015; Wang et al., 2016; Wang et al., 2018),  
42 hydrogen energy storage (Le Duigou et al., 2017; Ozarlan, 2012; Slizowski et al., 2017b),and  
43 particularly natural gas storage (Liu et al., 2018; Wang et al., 2013).

44 The usage of natural gas resources strongly fluctuates according to the season, while the gas  
45 well production is stable(Arfaee and Sola, 2014; Lawal et al., 2017). To balance the mismatch in gas  
46 supply and demand, in recent years, some countries have addressed the construction of large-scale  
47 storage caverns in salt rock formations (Evans and Chadwick, 2009; Le Duigou et al., 2017;  
48 Michalski et al., 2017; Parkes et al., 2018; Shi et al., 2017; Slizowski et al., 2017a). An appropriate  
49 leaching method is the key to successful construction of salt cavern gas storage. As it determines  
50 whether the cavern can meet the requirements of underground gas storage as well as the construction  
51 time of the salt cavern UGS, so it always the primary considered issues.

52 When the conventional single-well-oil-blanket method was used for the construction of a SWV  
53 cavern in salt formations, the construction efficiency is low and the usable volume of the cavern is  
54 small. To overcome the restrictions of SWV-cavern, two-well leaching method is proposed to cavern  
55 construction in the thinly bedded salt rocks. Based on the connecting method and the interwell  
56 distance, the two-well system leaching technology can be divided into TWV cavern technology and  
57 TWH cavern technology(Ban, 2017),as shown in Fig. 1 and Fig. 2.

58 The TWV cavern consists of two vertical wells. The wells are connected by the leaching  
59 method. This technology has already had engineering cases, such as the TA&TB UGS in Manosque,  
60 France (De Laguérie and Cambon, 2010) and the Zuidwending UGS in the Netherlands(WILKE et  
61 al., 2011).In contrast to the SWV cavern method, the construction rate of TWV cavern method is  
62 faster in the early stage. In the later stage, the cavern construction rate of these two methods are  
63 similar. Moreover, it is difficult to control the cavity shape with the TWV cavern method, especially  
64 for thinly-bedded salt formations with a low halite purity; and it is also difficult to build a larger

65 volume cavity using the TWV cavern method (Jiang et al., 2016a).

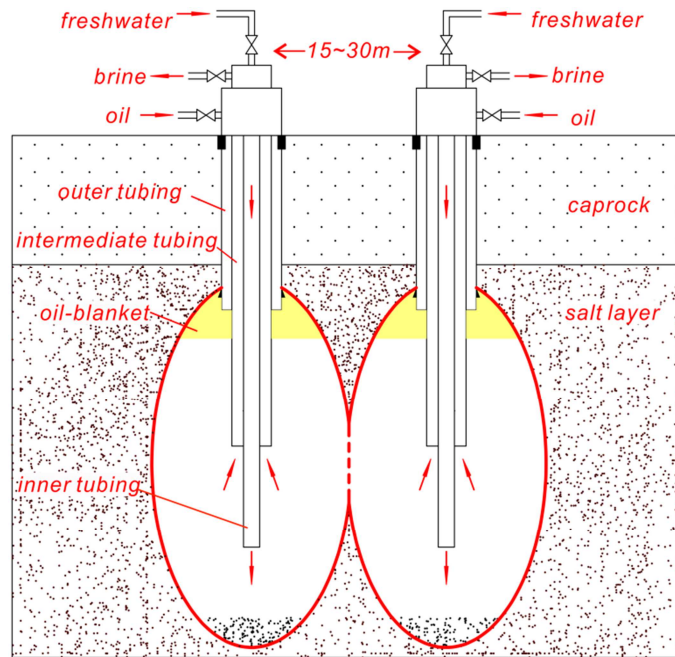


Fig. 1. Two-well-vertical (TWV) cavern

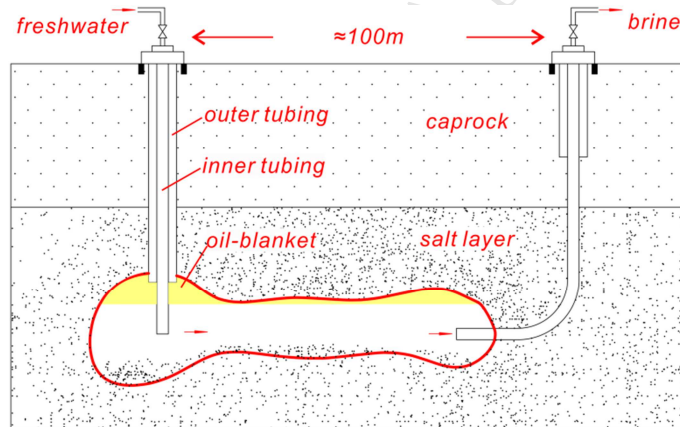


Fig. 2. Two-well-horizontal (TWH) cavern

66 The TWH cavern is constructed using a two-well system. The process consists of the following  
 67 steps: (i) drilling a vertical well and a horizontal well to the target salt formation, plus casing  
 68 cementing and the installation of the inner tubings. Then, directional installation technology is used  
 69 to connect the two wells; (ii) injecting fresh water from one inner tubing and extracting brine from  
 70 the other (Liu et al., 2018). The TWH cavern method can fully utilize the salt formation and allows  
 71 for the construction of a larger cavity. In contrast to SWV cavern and TWV cavern, TWH cavern has  
 72 several distinct advantages, such as higher adaptability to thin-bedded salt rocks, faster rate for  
 73 cavern construction, higher flexibility of operation, and lower stock of cushion gas. This method was  
 74 predominantly adopted for salt mining. In recent years, scholars have proposed the application of this

75 method to UGS construction (Bowen and Priestly, 1967; Russo, 1995). Until now, the sonar  
 76 surveying technique has been unable to measure a horizontal cavern's shape. Some researchers have  
 77 conducted physical simulation experiments to study the process of cavity expansion, but it is difficult  
 78 to get a precise distribution of the velocity field and brine concentration field (Jiang et al., 2016a;  
 79 Jiang et al., 2016b). Therefore, numerical simulation becomes an alternative way to obtain the  
 80 solution mining process for TWH caverns.

81 Since the 1960s, great progress has been made in the field of numerical simulation of solution  
 82 mining for UGS (Kunstman and Urbanczyk, 2000). For instance, a series of commercial cavern  
 83 leaching simulation codes have been developed. The algorithm can be divided into two categories:  
 84 floating plume (SANSMIC) (Russo., 1983) and balance principle (WinUbro) (Kunstman and  
 85 Urbanczyk, 2009).

86 **Floating plume:** In the floating plume method, the dissolved area is divided into four regions  
 87 by the floating plume algorithm according to the flow characteristics (boundary layer region, main  
 88 dissolution region, floating plume region, and dead water region). Concentration distribution and  
 89 cavern expansion in each region are calculated by different mathematical models. In the algorithm  
 90 turbulence is taken into account, the concept of floating plume is introduced, and the calculation is  
 91 simplified when combined with the engineering. However, the region division is too dependent on  
 92 experience, it is more arbitrary, and with the change of the cavern shape, the region division needs to  
 93 be manually adjusted.

94 **Balance principle:** In the balance principle method, the brine concentration field is simplified  
 95 into a horizontal layered distribution according to the balance principle algorithm. The cavern shape  
 96 is corrected through the mass conservation equation. Cavern expansion calculation can be quickly  
 97 achieved, and the results are corrected by a solution mining balance calculation. However, here the  
 98 concentration field is simplified and a large number of experimental data are in fact needed for solve  
 99 the cavern expansion.

100 Table 1 Differential salt cavern leaching simulation codes

Algorithm	Floating plume	Balance principle	N-S equation
Representative code	SANSMIC ( For 2D SWV)	WinUbro ( For 2D SWV)	Did not exist before
Development team	Sandia	Chemkop	Did not exist before

Computing method	1) The cavern is divided into four regions according to its flow characteristics. 2) Each region is calculated by a different mathematical model.	1) The concentration field is simplified into a horizontal layered distribution. 2) The cavern shape is corrected using the mass conservation equation.	1) Classical calculation method for fluid mechanics. 2) Based on the basic physical principles.
Advantages	1) Turbulence is taken into account. 2) Combined with engineering, the calculation is simplified.	1) The cavern expansion calculation can be quickly achieved. 2) Results are corrected using balance calculation.	1) With the good generality, the flow-mass transfer in each area and stage can be described effectively and uniformly. 2) Beside the basic physical parameters of rock salt, no empirical data are required. 3) Can provide more refined results for more variables.
Disadvantages	1) Region division is too dependent on experience. 2) With the cavern shape change, region division needs to be adjusted manually.	1) Concentration field is simplified and a lot of experimental data are needed to solve the cavern expansion.	1) Geometric modeling and meshing are more complicated. 2) A dense grid and more complex equations lead to greater computing resource consumption and longer calculation time.

101 As shown in the Table 1, the existing commercial codes based on the floating plume method  
102 and the balance principle method are only applicable to the 2D simulation of the SWV cavern  
103 working condition. However, during the leaching process of the TWH cavern in thin salt beds, both  
104 the geometry and the mass transfer process are more complex, thus, until now there has been no  
105 commercial code applicable to the leaching process of TWH caverns.

106 The N-S equation method is the classical calculation method for fluid mechanics. Based on  
107 basic physical principles, the flow mass transfer phenomenon is described for the entire cavern in the  
108 actual 3D area without artificial zone division. The 3D calculation ability and the uniform processing  
109 of this method in space avoid deviations from geometric simplification and geometric partitioning. It  
110 can effectively describe the flow and mass transfer for each area and stage effectively and uniformly.  
111 The N-S equation method is based on the basic principle of flow and mass transfer, thus the physical  
112 picture of the calculation is clearer. And no empirical data is required, while more refined results for  
113 more variables can be provided. In principle, we can use the N-S equation to describe flow and mass  
114 transfer as well as the boundary movement problem without any constraints. At the same time, the  
115 3D computational domain and 3D discretization required by the method lead to complicated  
116 geometric modeling and meshing. And there are a large number of equations need to be solved, so  
117 more computing resource and longer calculation time is required.

118 During the construction of salt cavern UGSs, the shapes of the caverns are always the primary  
119 issues considered. However, FLUENT, CFX and other CFD codes (Fluent, 2012) are professional  
120 commercial software packages based on the N-S method, only used in the flow simulation under a  
121 fixed cavity shape. Thus, these CFD codes cannot describe the movement of the boundary of the  
122 cavern, they are not competent to simulate the cavity dissolution process.

123 For the further development of the TWH salt cavern gas storage, in this study, based on the  
124 basic principles of the N-S equation method and using some reasonable assumptions, we established  
125 a 3D mathematical model of the flow-mass transfer and boundary movement. We developed a  
126 VC++ computer code program (TWHSMC) that provides a numerical solution of the model, in  
127 addition to the velocity field, brine concentration field, cavern volume and cavern shapes. We  
128 selected an engineering case and the leaching process is simulated by the developed program. The  
129 comparison of the simulation results with the experimental data demonstrates the validity and  
130 accuracy of the proposed model. This study reveals the characteristics of the TWH cavern leaching  
131 process and supplies theoretical useful guidance for TWH salt cavern storage construction.

## 132 **2. Methodology**

133 The dissolution process of rock salt is the transport process of solute in the solvent flow system.  
134 This process is a complex fluid dynamics and chemical kinetics process. Based on the dynamic  
135 analysis of the 3D convection and diffusion process, combined with the basic theory of fluid  
136 mechanics, chemical kinetics, and thermodynamics principles, a mathematical model of solute  
137 transport and fluid flow in the process of solution mining can be established. In this way the  
138 mechanism of dissolving rock salt can be studied.

139 The dissolution process of rock salt is actually the diffusion process of rock salt molecules in  
140 water. The diffusion effect was produced by gradient change in concentration. The molecules spread  
141 from the high concentration area to lower concentration area depending on thermal motion, and  
142 finally tend to wards equilibrium. The diffusion occurs even when there is no macro flow.

143 The dissolution process and diffusion process of salt in brine is consistent with the dissolution  
144 mechanism of rock salt. For convenience, the dissolution process of salt rock can be simplified as



145 follows: As shown in Fig. 3, the salt molecules dissolve from the solid rock salt into the diffusion  
 146 zone through the boundary layer, and the total amount of substances in the boundary layer has  
 147 always maintained the dynamic balance between dissolution and diffusion.

148 As such, the dissolution process can be divided into the following 3 steps:

149 (1) The rock salt molecules in the boundary layer diffuse into the flow field, decreasing the  
 150 concentration of the boundary layer.

151 (2) The solid rock salt wall's surface dissolves, and the rock salt molecules then enter the  
 152 boundary layer to replenish its substantial loss, so such the concentration of the boundary layer is  
 153 compensated by rising again.

154 (3) Due to the dissolution of salt solid wall, the wall (along with the attached boundary layer)  
 155 recedes a small distance  $dR$ .

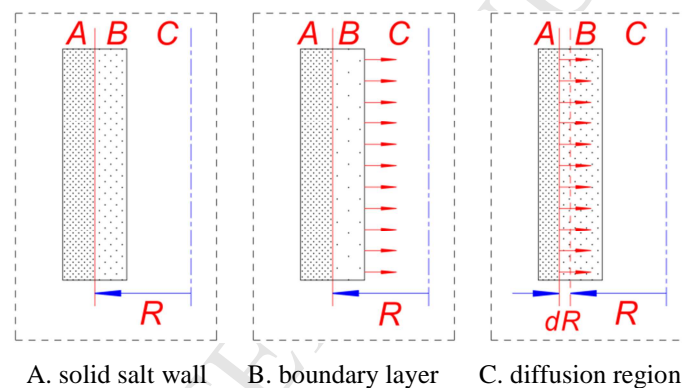


Fig. 3. Sketch of salt rock dissolving process

156 In this section, the control equations of fluid flow and mass transfer are derived, as well as the  
 157 equations for the development of the cavern boundary. In this way, we propose the definite solution  
 158 conditions and solving algorithm of the mathematical model. Based on the model and the algorithm,  
 159 we created a software program for TWH solution mining.

## 160 2.1. Assumptions

161 In previous studies on numerical simulations of solution mining for UGS, the problem was  
 162 simplified for the calculation, and the assumptions have generally been proposed as follows(Ban et  
 163 al., 2006; Zhicheng et al., 2004):

164 (1) The influence of microstructure anisotropy (stratigraphic dip, salt crystal direction, bedding,

165 etc.) on the rock salt dissolution process is neglected.

166 (2) Insolubles are 100% precipitated and their effect on diffusion is neglected.

167 (3) The influence of temperature difference is neglected.

168 (4) The cavern structure is axisymmetric and a two-dimensional model is adopted.

169 (5) The concentration of the boundary layer is saturated.

170 (6) Concentration and density are the unary functions of height.

171 In the simplification of this mathematical calculation, each additional assumption increases the  
172 deviation from reality. In order to enhance the practicability and accuracy of the program, the  
173 mathematical model of this study minimizes these assumption, and only assumptions (1)–(3) are  
174 retained. Every cancellation of an assumption is therefore relatively progressive and innovative.

175 In this study, a 3D model was used to achieve a true geometric simulation, and the distributions  
176 of the velocity field and the concentration field were solved directly. Assumptions were corrected as  
177 follows.

178 (1) The influence anisotropy on the microstructure on the rock salt dissolution process is  
179 neglected, such as stratigraphic dip, salt crystal direction, bedding, etc.

180 (2) Insolubles are 100% precipitated and their effect on diffusion is neglected.

181 (3) The influence of temperature difference is neglected.

## 182 2.2. Fluid flow and mass transfer equations

183 The governing equations of flow, mass transfer and dissolution during the solution mining  
184 process are as follows:

185 (1) Continuity equation

186 According to the law of mass conservation and the Reynolds equation, the continuity equation  
187 can be expressed as.

$$\frac{\partial \rho}{\partial t} + \nabla \cdot (\rho u) = 0 \quad (1)$$

188 Where  $u$  is the speed vector.

189 (2) Momentum equation

190 According to the N-S equations, the fluid momentum equation can be written as

$$\frac{\partial u}{\partial t} + (u \cdot \nabla)u = f - \frac{1}{\rho} \nabla P + \nu \nabla^2 u \quad (2)$$

191 where  $\nu$  is the kinematic viscosity,  $\nabla P$  is the pressure gradient,  $P$  is the average dynamic  
192 pressure, and  $f$  is a unit mass force vector.

193 When the mass force is only gravity, equation (4.2) can be written as

$$\frac{\partial u}{\partial t} + (u \cdot \nabla)u = -g \nabla h - \frac{1}{\rho} \nabla P + \nu \nabla^2 u \quad (3)$$

194 where  $h$  is the vertical coordinate (upward is positive).

195 (3) Concentration equation

196 The dissolution process of rock salt is actually the diffusion process of rock salt molecules in  
197 solvent. It can be described by the convection-diffusion equation.

$$\frac{\partial C}{\partial t} + (u \cdot \nabla)C = D \nabla^2 C \quad (4)$$

198 Where  $C$  is the molar concentration, and  $D$  is the diffusion coefficient.

199 (4) The diffusion can be described by Fick's first law of diffusion,

$$J = -D \frac{\partial C}{\partial n} \quad (5)$$

200 Where  $J$  represents the diffusion flux. That is, the mass flow of matter through a unit area  
201 perpendicular to the normal direction.  $\vec{n}$  is normal vector.

202 (5) Auxiliary equation

203 In the dissolution process of rock salt, due to the flow of brine and solute diffusion, the  
204 concentration of the fluid system is constantly changing—so the density is also changing. The  
205 relationship between density and concentration can be thus written as.

$$r = r_w + CM \left( \frac{r_w}{r_s} - 1 \right) \quad (6)$$

206 Where  $r_w$  represents the density of distilled water. The variable  $r_s$  represents the density of  
207 rock salt, and  $M$  represents the molar mass of rock salt.

## 208 2.3. Mathematical model of boundary movement

209 As the rock salt dissolves, its boundaries move toward the interior of the solid domain (away  
 210 from the solution). The dissolution rate model in this section relates the dissolution rate and the rock  
 211 wall direction to the brine concentration. Based on the model, the moving speed of rock salt wall  
 212 boundary can be quantified. Referring to the VOF method in the CFD simulation of the two-phase  
 213 flow, this study proposes a numerical algorithm based on the finite volume method for boundary  
 214 movements, which computes the numerical solution of the rock wall boundary movement using a  
 215 fixed grid.

216 Our analysis of the characteristics of fluid transport in the mining salt cavern solution, reveals  
 217 that the rock salt dissolution process manifests as the exchange of matter in the boundary layer. The  
 218 basic process is molecular diffusion. Under the action of diffusion, the salt molecules dissolved from  
 219 the wall's surface enter the solution through the boundary layer. The rate of molecular diffusion is  
 220 also related to the concentration of the boundary layer.

221 The relationship between dissolution rate and concentration of boundary is

$$flux|_{G_i} = k(C_s - C) \quad (7)$$

222 During the process of solution mining, the dissolution rates of rock salt are divided into rate for  
 223 the upper solution, side solution and bottom solution. Considering insoluble deposition at the bottom,  
 224 we assume the bottom solution rate to be zero.

225 Table 2 Anisotropic dissolution rates in the cavity (Xue, 1994)

Concentration( g / l )	Dissolution rate( kg / m <sup>2</sup> · h )	
	Upper	Side
0	41.4	21.2
112	26.0	14
250	4.1	2.5

226 According to the above experimental results, the dissolution rate formula for different  
 227 directions was obtained by fitting:

228 1) Formula for the rate of upper solution:  $flux|_{G_i} = - 0.1496C + 41.88$

229 2) Formula for the rate of side solution:  $flux|_{G_i} = - 0.0751C + 21.632$

230  $C_s$  is the saturation concentration of brine,  $\Gamma_1$  represents the surrounding sidewall (the upper  
 231 and side surfaces only) of the cavern,

## 232 2.4. Definite conditions

233 The above equations can only be solved with the proper initial and boundary conditions.  
 234 According to the engineering, the definite conditions can be defined as follows.

### 235 (1) Initial conditions

236 Before the salt dissolution, the aqueous solution that makes contact with the rock salt boundary  
 237 is stationary, so the initial conditions can be expressed as

$$238 \quad V|_{t=0} = 0, C|_{t=0} = C_0$$

### 239 (2) Boundary conditions

240 For  $\Gamma_1$ , there is a no-slip boundary condition,

$$241 \quad V|_{\Gamma} = 0,$$

242 the bottom surface of the cavern is impermeable,

$$243 \quad \left. \frac{\partial C}{\partial n} \right|_{\Gamma_2} = 0,$$

244 And the solution mining system is considered to have a constant formation temperature,

$$245 \quad T|_{\Gamma=0} = T_0.$$

246 where  $C_0$  represents the molar concentration of the aqueous solution in the initial state.  $\Gamma_1$   
 247 represents the surrounding wall of the cavern, and  $\Gamma_2$  represents the bottom surface of the cavern.

## 248 2.5 Numerical algorithms

249 In this calculation, we used the SIMPLE Algorithm for flow and mass transfer and the  
 250 Boundary Movement Algorithm based on VOF.

251 2.5.1 The SIMPLE Algorithm

252 The SIMPLE algorithm is a numerical method primarily used to solve incompressible flow  
 253 fields. Its core advantage is to use the process of "guess-correction" to calculate the pressure field on  
 254 the basis of the staggered grid, so as to solve the momentum equation (N-S equations). The  
 255 calculation process is shown in Fig. 4.

256 2.5.2 Boundary Movement Algorithm

257 The basic principle of the VOF method is to determine the solid-liquid interface and track the  
 258 change of the fluid by studying the mesh volume ratio function  $F$  of the fluid in the grid unit. The  
 259 VOF method defines this function for the entire flow field. In each grid, the function is defined as the  
 260 ratio of the volume of a fluid (the target fluid) to the volume of the grid.

261 Assuming that the calculation area is recorded as  $\Omega$ , the area where the fluid is recorded as  
 262  $\Omega^A$ , the area where solid is recorded as  $\Omega^B$ , then  $\alpha(\bar{x}, t)$  is defined as a function,

$$\alpha(\bar{x}, t) = \begin{cases} 1 & \bar{x} \in \Omega^A \\ 0 & \bar{x} \in \Omega^B \end{cases} \quad (8)$$

263 where,  $\alpha(\bar{x}, t)$  satisfies the characteristics of the Lagrangian fluid volume,

$$\frac{\partial \alpha}{\partial t} + u \frac{\partial \alpha}{\partial x} + v \frac{\partial \alpha}{\partial y} + w \frac{\partial \alpha}{\partial z} = 0 \quad (9)$$

$$F_{ij} = \frac{1}{\Delta V_{ij}} \int_{I_{ij}} \alpha(\bar{x}, t) dV \quad (10)$$

264 where  $\Delta V_{ij}$  is the volume of a single grid.  $F_{ij}$  is defined as the integral of  $\alpha(\bar{x}, t)$  for each  
 265 grid,  $I_{ij}$ .

266 The above formula is a VOF function, and it also satisfies:

$$\frac{\partial F}{\partial t} + u \frac{\partial F}{\partial x} + v \frac{\partial F}{\partial y} + w \frac{\partial F}{\partial z} = 0 \quad (11)$$

267 It can be seen from the above that the volume function for each fluid is essentially:

$$F = \frac{\text{Fluid volume in the grid}}{\text{Grid volume}}$$

268

269 Obviously, when  $F = 1$ , the grid is filled with fluid A, which we call *fluid grid*. When  $F = 0$ , it  
 270 is solid grid. When  $0 < F < 1$ , it is a grid with a fluid interface called an *interface grid*.

271 According to the distribution of the  $F$  function over the whole calculation domain, the  
 272 solid-liquid interface (i.e., the cavity contour) can be obtained by constructing the isosurface of the  $F$   
 273 function. Then, when solving the physical equation, special fine processing can be performed near  
 274 the interface to improve resolution and accuracy. Since each grid only needs to store one  $F$  value, it  
 275 can greatly reduce the amount of storage.

276 The Boundary Movement Algorithm consists of two steps: first, calculating the boundary  
 277 movement of the top and side surfaces caused by the dissolving the rock salt, and secondly,  
 278 calculating the bottom surface boundary movement caused by the insoluble substance deposit at this  
 279 stage.

#### 280 (1) Calculation process of solid wall grid dissolution

281 This process defines the amount of dissolution for current solid wall to be  $dV$  per day; a single  
 282 mesh volume is  $V$ . If  $dV \leq V$ , the mesh boundary moves. If  $dV > V$ , the current mesh dissolution is  
 283 complete and hence dissolves the next layer in all directions. The calculation process is shown in Fig.  
 284 5.

285 In the dissolution process of the solid wall, the changes of various mesh types and VOF  
 286 functions can be divided into several stages as shown in Fig. 6.

#### 287 (2) Calculation process of the insoluble substance deposit

288 This process defines the total volume of insoluble substance of the fallen solid wall as  $V_s$ ,  
 289 while the total volume of fluid in the current layer of the solid wall grid is  $V_f$ . When  $V_s \leq V_f$ , all solid  
 290 wall grids in this layer move synchronously. When  $V_s > V_f$ , it indicates that the grid of the current  
 291 layer is filled, and that the next layer will also be filled until all insoluble substances have settled.  
 292 The calculation flowchart of the insoluble substance deposit is shown in Fig. 7.

## 293 2.6. Program development

294 Based on the continuity equation, momentum equation, convection-diffusion equation, Fick's  
 295 first law of diffusion equation, the auxiliary equation, and the definite solution conditions, the final

296 governing partial differential equations of the solution mining model are obtained.

297 As the numerical model was established, the numerical solution was performed on a computer.  
298 For this purpose, the numerical simulation application code “TWH solution mining cavern”,  
299 “TWHSMC” for short, of the TWH cavern is developed to solve the numerical solution of the model.  
300 Using the finite volume method, TWHSMC was written in the VC++ language. The flowchart of the  
301 program is shown in Fig. 8 and Fig. 9, and the independent operation interface is shown in Fig. 10.  
302 There are five function modules in TWHSMC: a) formation information import, b) technical  
303 parameter input, c) flow/concentration field calculation, d) cavern boundary calculation, and e)  
304 insoluble sediment calculation.  
305



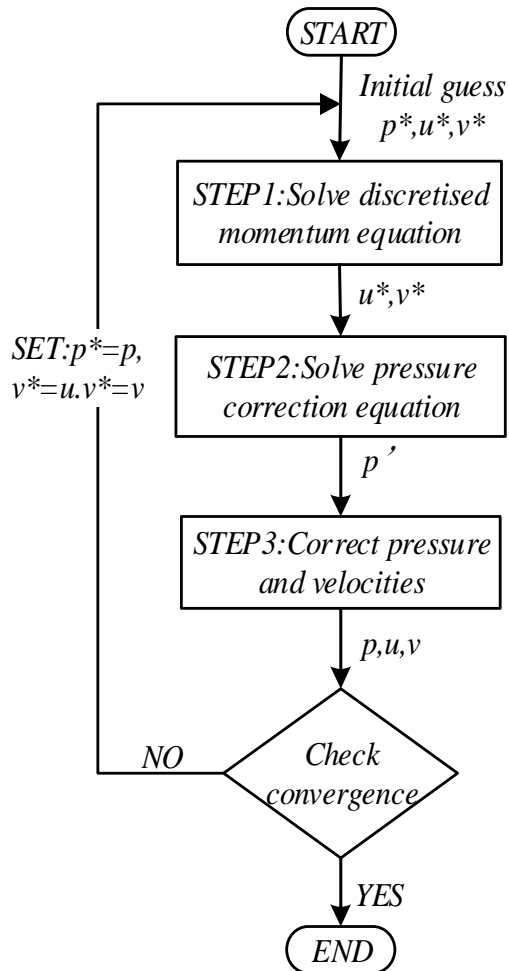


Fig. 4. Flow chart of the SIMPLE algorithm

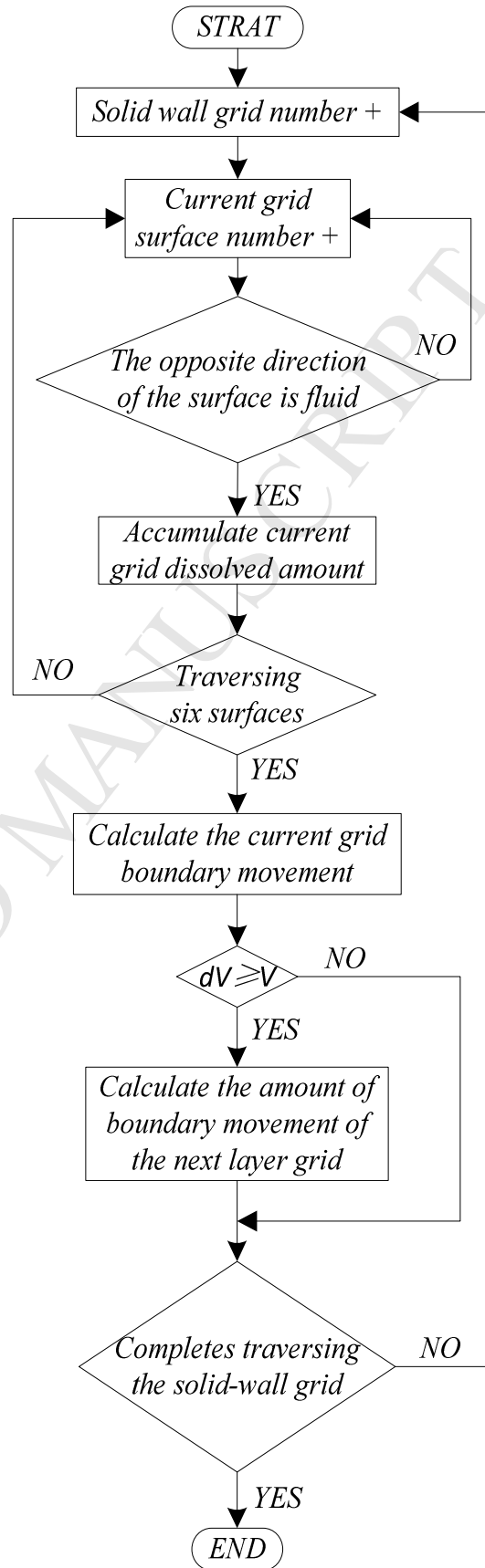
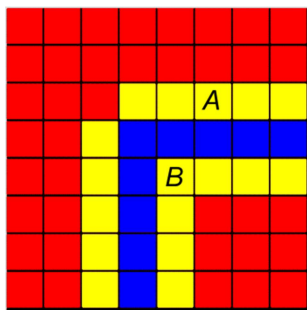
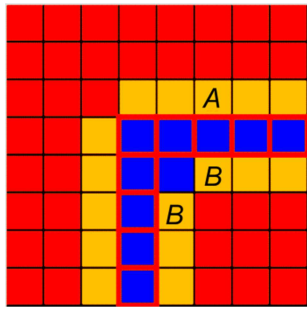


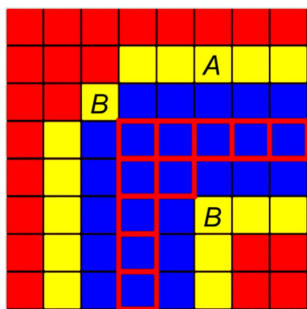
Fig. 5. Calculation flowchart for solid wall mesh dissolution



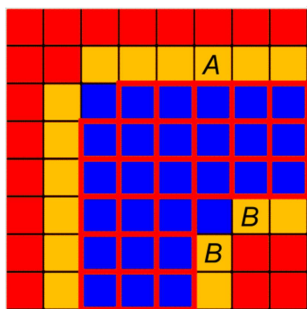
State 1



State 2



State 3



State 4

Fig. 6. Changes of various mesh types

*Notice: the dark red grid represents the solid area. The dark yellow grid represents the solid wall with a large VOF value. The pale yellow grid represents the solid wall with a small VOF value. The blue area represents the fluid. The dark red wireframe represents the fluid area in the previous step.*

Fig. 7. Calculation flow chart of insoluble substance deposit

Fig. 8. Flowchart of pre-processing

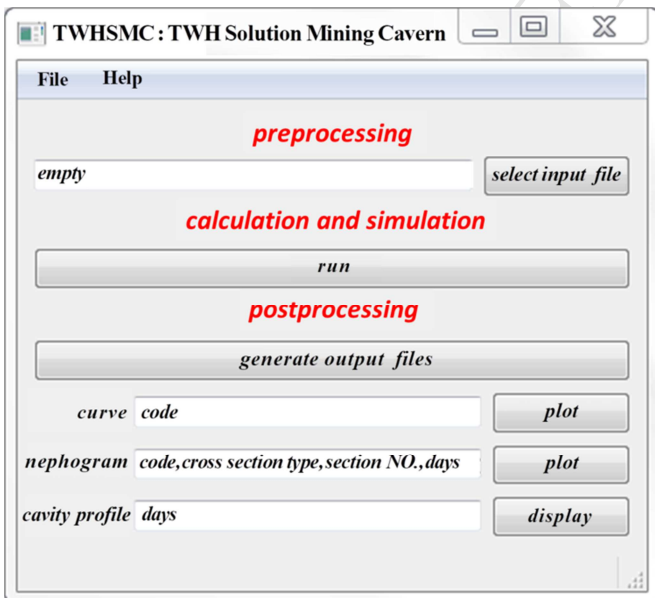


Fig. 10. Program graphical user interface

Fig. 9. Flowchart of the simulation of cavern leaching by TWHSMC

### 306 3. Case study and results

307 In this section we simulate the leaching process of a complete salt cavern, using reasonable  
 308 geological and technological parameters, and then compare the simulation results with the cavern  
 309 shape of the physical experiment to verify the model.

#### 310 3.1. Computational case

311 We assume an idealized TWH cavern model, in which the values of the geometrical and  
 312 physical properties of the reservoir are referenced from the values employed in previous numerical  
 313 studies on typical rock salt UGS projects (Ban et al., 2006; Zhicheng et al., 2004), as shown in Fig. 11  
 314 and Table 3.

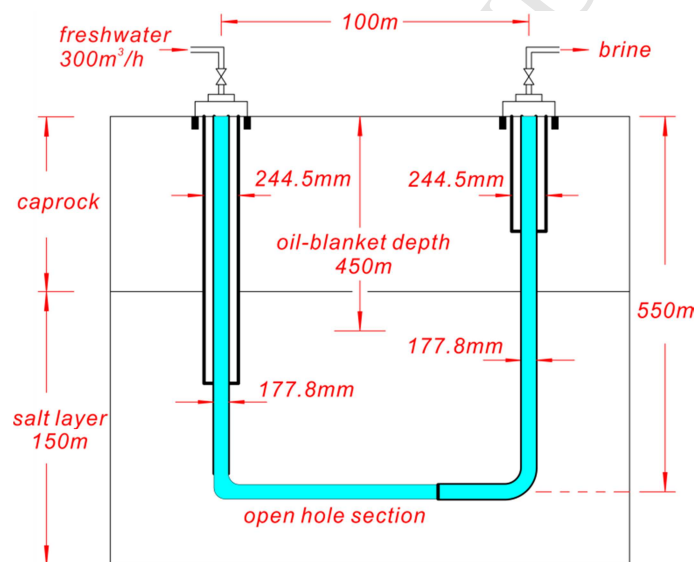


Fig. 11. Schematic diagram of the calculation case

315 Table 3 Basic parameters of numerical experiments

Formation parameters		Geometry parameters		Working condition			
Thickness	150m	Interwell distance	100m	Oil-blanket depth	450m		
Density	2163 kg/m <sup>3</sup>	Initial well depth	550m	System temperature	45℃		
Insolubles expansion coefficient	1.2	Casing diameters	Outer	244.5mm	Water injection	Method	One-way
Insolubles percentage	15%		Inner	177.8 mm		Flow rate	300m <sup>3</sup> /h

### 316 3.2. Velocity distribution

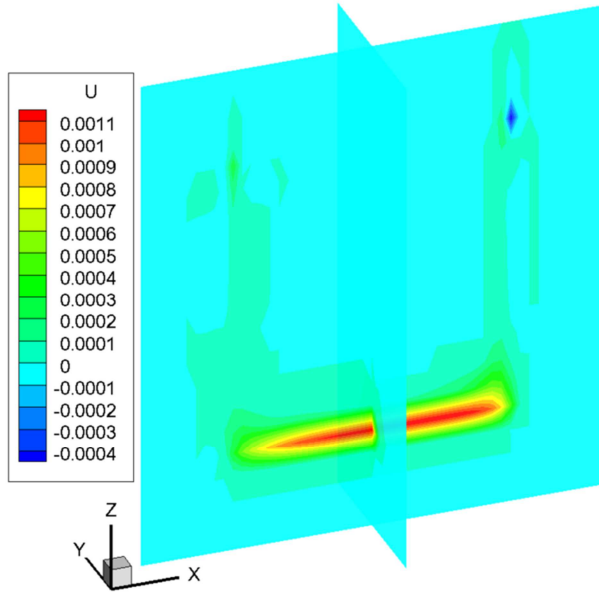


Fig. 12. t= day 100, X-direction velocity distribution

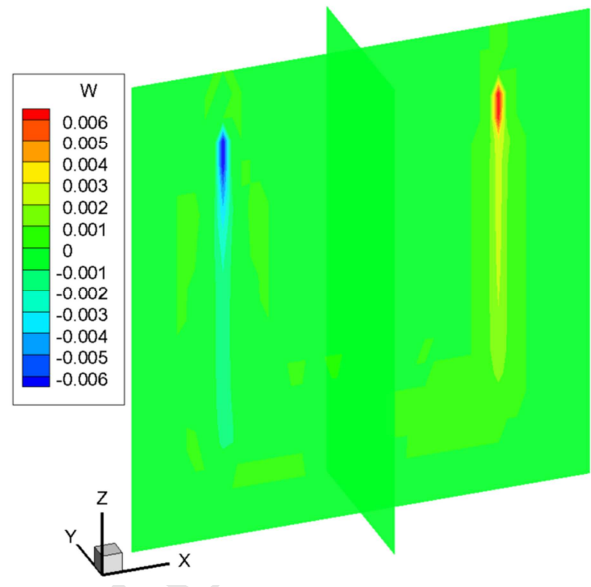


Fig. 13. t= day 100, Z-direction velocity distribution

317 As shown in Fig. 12, the horizontal well section has a strong flow from injection well to  
 318 withdrawal well, driven by the pressure differential between them.

### 319 3.3. Concentration distribution

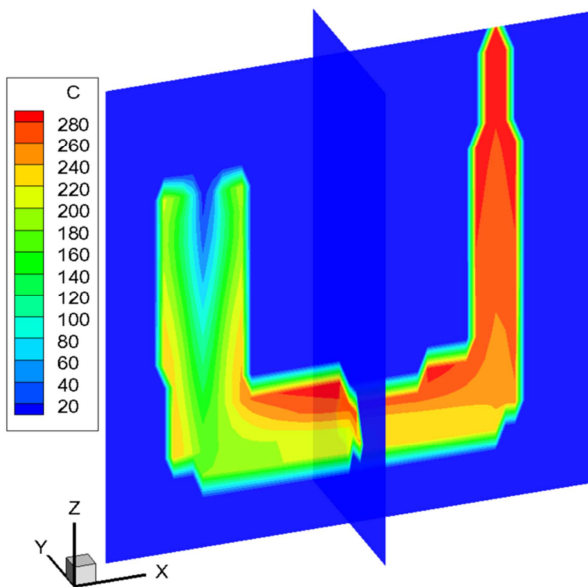


Fig. 14. t= day 100, concentration distribution

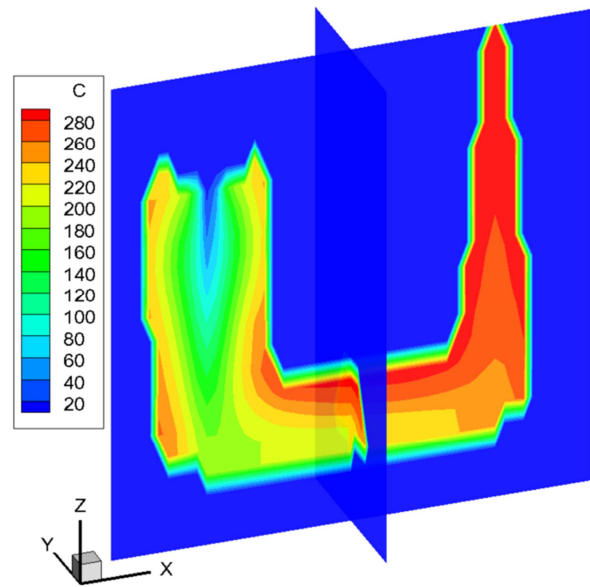


Fig. 15. t=day 200, concentration distribution

320 According to the concentration distribution (Fig. 14 and Fig. 15), near the injection well, the  
 321 rock salt that dissolves is mainly near the dissolution starting point. The concentration distribution of

322 brine is affected by gravity, so the deeper brine have higher concentrations. Thus, the brine that  
 323 squeezes into the horizontal well section has a higher concentration, reducing the dissolution. During  
 324 the flow in the horizontal channel, the brine concentration continues to increase, and it tends to be  
 325 saturated when reaching the wellhead of the withdrawal well.

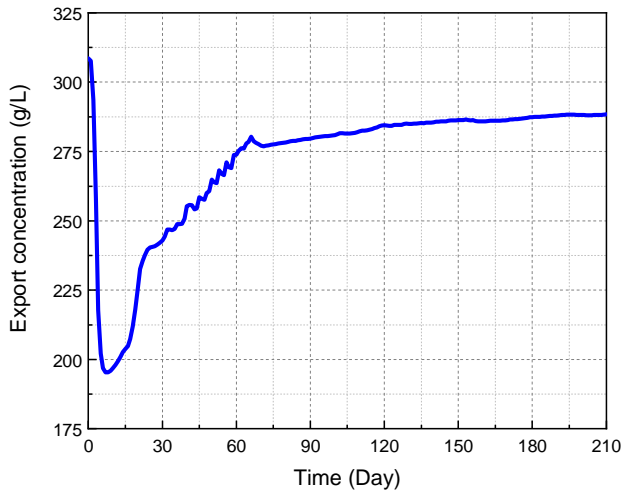


Fig. 16. Concentration-time curve of the numerical simulation

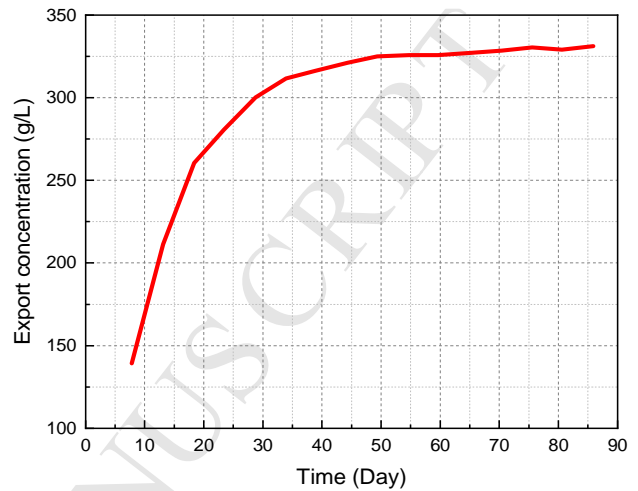


Fig. 17. Concentration-time curve of the experimental simulation(Liu et al., 2017)

326 Comparing the numerical simulation results(Fig. 16) with the experimental result(Fig. 17) (Liu  
 327 et al., 2017), under similar conditions, we see that the numerical simulation for the  
 328 concentration-time curve of the withdrawal well is consistent with the experimental one, hence  
 329 supporting the validity of the code.

330 Due to the brine in the cavern is saturated in the initial state, the brine of export has a higher  
 331 concentration. With the injection of fresh water, the concentration in the chamber gradually  
 332 decreases, and the outlet concentration dropped to about 200 g/L. And then export concentration  
 333 rises rapidly and gradually stabilizes. This is because the initial dissolution area of the TWH cavern  
 334 is relatively large. When the concentration reaches a certain level, the concentration growth rate  
 335 slows down and the curve tends toward the horizontal, indicating that the water injection flow rate  
 336 and the dissolution rate are near equilibrium. That is, high concentrations protect the deeper rock salt  
 337 from over-dissolving.

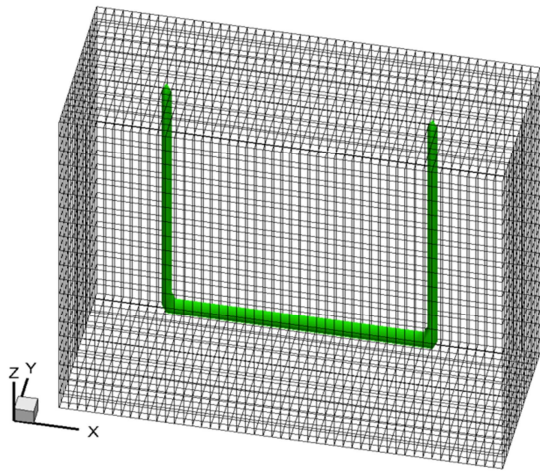
338 **3.4. Numerical process of cavern expansion**

Fig. 18. Initial shape of cavern

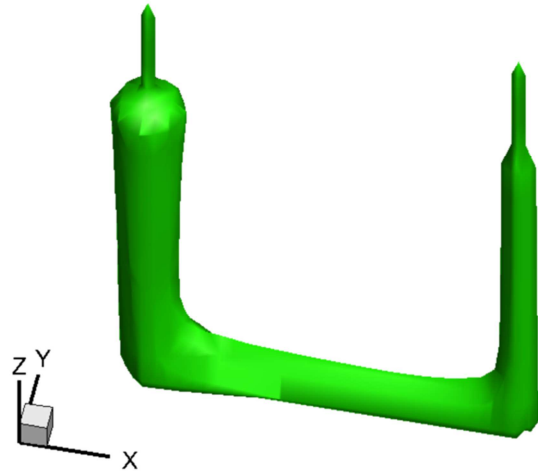


Fig. 19. Cavern shape, t= day 50

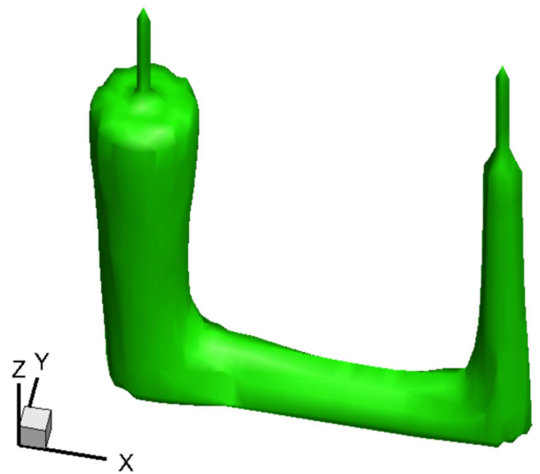


Fig. 20. Cavern shape, t=day 100

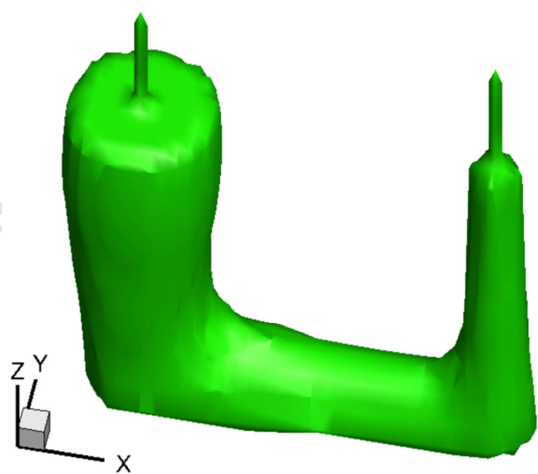


Fig. 21. Cavern shape, t=day 200

339

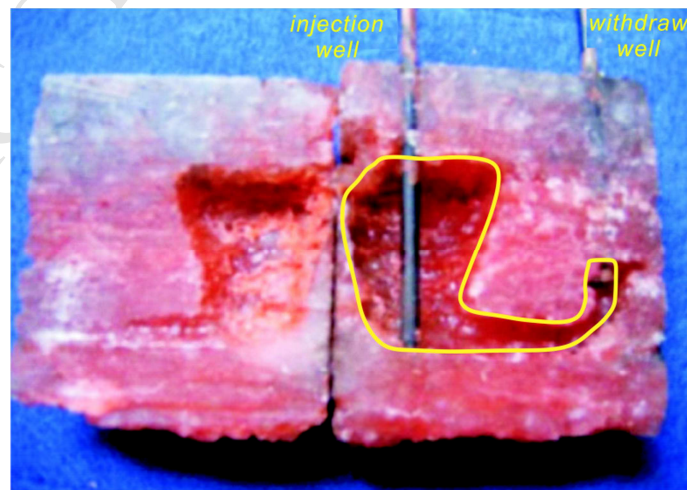


Fig. 22. TWH cavern shape of experimental simulation under one-way water injection(Zheng et al., 2018)

340 The Fig. 22 shows the TWH cavern cross-sectional shape for the experimental simulation  
 341 under one-way water injection(Zheng et al., 2018). The numerical cavern shapes agree with the  
 342 experimental simulation, indicating that the numerical simulation method is effective.

343 The results of the numerical simulation and experimental simulation, show that the TWH  
 344 cavern shape under one-way water injection is very asymmetric. Near the water injection well, the  
 345 dissolving cavity is large, and it mainly dissolves upwards in the early stage, and only dissolves the  
 346 surrounding sides in the later stage. The injection well cavity forms a similarly inverted truncated  
 347 cone shape, which is wide at the top and narrow at the bottom. Near the brine withdrawal well, the  
 348 cavity construction rate is slow, so the cavity is small; and the cross-sectional area of the horizontal  
 349 section gradually becomes smaller.

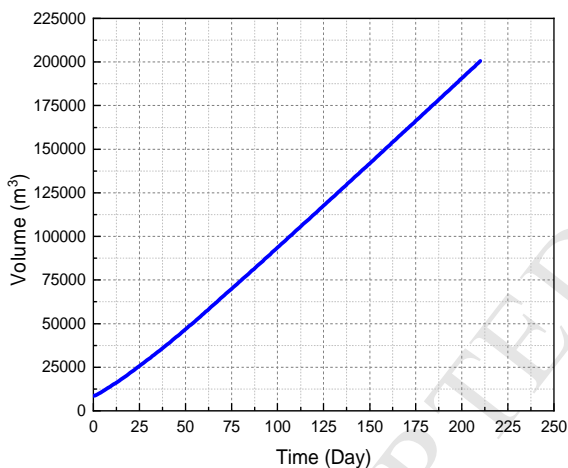


Fig. 23. Volume-time curve of TWH cavern construction

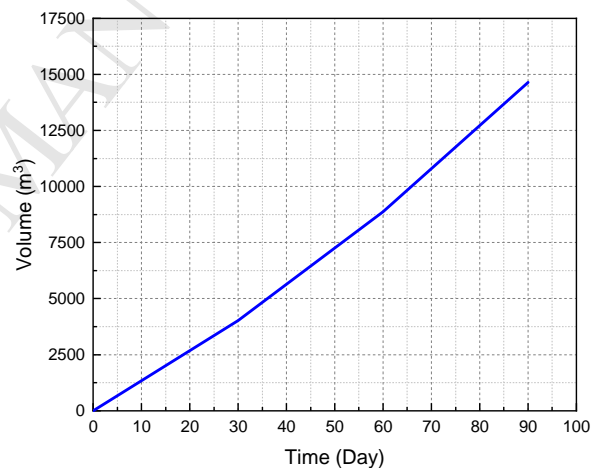


Fig. 24. Volume-time curves of SWV-cavern construction(Zhicheng et al., 2004)

350 According to numerical simulation for the SWV cavern(Zhicheng et al., 2004), one-way water  
 351 injection was used to construct a cavern, and 90days were required to achieve a volume of  $14636 m^3$ .  
 352 Compared with the numerical simulation for the TWH cavern in this study, the SWV case only  
 353 needed 22 days to achieve the same volume, thus the cavern constructing rate is increased by a factor  
 354 of 4.09.

## 355 4. Conclusion

356 The main results and conclusions obtained in the study are as follows:



357 (1) Comparison between TWH and SWV cavern construction, shows that the concentration of  
358 brine rises more rapidly during for TWH. In addition, the volume of the salt cavern that can be built  
359 is larger. Thus, the TWH cavern method has great potential to be used in UGS storage construction.

360 (2) The TWH cavern shape under one-way water injection is very asymmetric, as shown in the  
361 model. It may lead to excessive dissolution near the injection well, and the span of the solution  
362 cavity may exceed the limit, which could present a geohazard such as ground subsidence. Therefore,  
363 in the process of TWH cavern construction, the concentration and flow rate of the brine should be  
364 monitored in real time, and the injection and withdrawal wells should be alternated according to the  
365 working conditions, so that the dissolution cavern can develop as evenly as possible.

366 (3) The best prediction process for solution mining cavern construction is an effective  
367 combination of numerical calculations and experimentation. Therefore, the integrated analysis of  
368 numerical and experimental simulation should be carried out in order to understand the mechanism  
369 of solution mining cavern construction in layered rock salt. It is important to further improve the  
370 reliability of the numerical simulation results as this is the most important direction of development  
371 for solution mining cavern construction simulation technology in the future.

## 372 **Acknowledgements**

373 The authors would gratefully like to acknowledge the financial support from the Beijing  
374 Science and Technology Development Fund Project (No.Z111100059411024) and PetroChina  
375 Science and Technology Major Project (No. 2015E-4003). The English text was reviewed and  
376 revised by Grant George Buffett.

## 377 **References**

- 378 Aghahosseini, A. and Breyer, C., 2018. Assessment of geological resource potential for compressed  
379 air energy storage in global electricity supply. *Energy Conversion and Management*, 169:  
380 161-173.
- 381 Arfaee, M.I.R. and Sola, B.S., 2014. Investigating the effect of fracture–matrix interaction in  
382 underground gas storage process at condensate naturally fractured reservoirs. *Journal of*  
383 *Natural Gas Science and Engineering*, 19: 161-174.
- 384 Ban, F., 2017. Status and development trend of solution mining technologies used for salt-cavern

- 385 gas storage. *Oil & Gas Storage & Transportation*, 36(7): 754-758.
- 386 Ban, F.S., Geng, J., Gao, S.S. and Shan, W.W., 2006. Studying on basic theory and influence factor of  
387 gas storage in salt caverns building with water solution. *Natural Gas Geoscience*, 17(2):  
388 261-266.
- 389 Bowen, D. J., & Priestly, E. B. (1967). U.S. Patent No. 3,347,595. Washington, DC: U.S. Patent and  
390 Trademark Office.
- 391 Budny, C., Madlener, R. and Hilgers, C., 2015. Economic feasibility of pipe storage and underground  
392 reservoir storage options for power-to-gas load balancing. *Energy Conversion and  
393 Management*, 102: 258-266.
- 394 De Laguérie, P. and Cambon, J.-L., 2010. Development of new liquid storage caverns at GEOSSEL  
395 MANOSQUE, Proc. SMRI Fall Meeting, Leipzig, Germany, pp. 161-174.
- 396 Evans, D.J. and Chadwick, R.A., 2009. Underground gas storage: An introduction and UK perspective.  
397 In: D.J. Evans and R.A. Chadwick (Editors), *Underground Gas Storage: Worldwide Experiences  
398 and Future Development in the UK and Europe*. Geological Society Special Publication.  
399 Geological Soc Publishing House, Bath, pp. 1-11.
- 400 Fluent, A., 2012. 14.5, theory guide; ansys. Inc., Canonsburg, PA.
- 401 Jiang, D.-Y., Yi, L., Chen, J., Ren, S. and Li, Y.-P., 2016a. Comparison of cavern formation in massive  
402 salt blocks with single-well and two-well systems. *Journal of the Chinese Institute of  
403 Engineers*, 39(8): 954-961.
- 404 Jiang, D.-Y. et al., 2016b. Laboratory similarity test relevant to salt cavern construction in  
405 interlayer-containing moulded saliferous aggregates specimen. *Current Science (00113891)*,  
406 111(1).
- 407 Kunstman, A. and Urbanczyk, K., 2000. Computer models of the salt cavern leaching process—  
408 evolution over the last 35 years. *Salt 2000*, 8-th World Salt Symposium.
- 409 Kunstman, A. and Urbanczyk, K., 2009. Application of winubro software to modelling of carven  
410 development in trona deposit, Solution Mining Research Institute Technical Conference,  
411 Krakow, Poland.
- 412 Lawal, K.A., Ovuru, M.I., Eytayo, S.I., Matemilola, S. and Adeniyi, A.T., 2017. Underground storage as  
413 a solution for stranded associated gas in oil fields. *Journal of Petroleum Science and  
414 Engineering*, 150: 366-375.
- 415 Le Duigou, A., Bader, A.G., Lanoix, J.C. and Nadau, L., 2017. Relevance and costs of large scale  
416 underground hydrogen storage in France. *International Journal of Hydrogen Energy*, 42(36):  
417 22987-23003.
- 418 Liu, J., Jiang, D., Jie, C. and Liu, X., 2017. Similar experimental construction and long-term stability  
419 analysis of horizontal salt caverns. *Journal of Chongqing University*.
- 420 Liu, W. et al., 2016. Tightness and suitability evaluation of abandoned salt caverns served as  
421 hydrocarbon energies storage under adverse geological conditions (AGC). *Appl. Energy*, 178:  
422 703-720.
- 423 Liu, W. et al., 2018. Comprehensive feasibility study of two-well-horizontal caverns for natural gas  
424 storage in thinly-bedded salt rocks in China. *Energy*, 143: 1006-1019.
- 425 Michalski, J. et al., 2017. Hydrogen generation by electrolysis and storage in salt caverns: Potentials,  
426 economics and systems aspects with regard to the German energy transition. *International*

- 427 Journal of Hydrogen Energy, 42(19): 13427-13443.
- 428 Ozarlsan, A., 2012. Large-scale hydrogen energy storage in salt caverns. International Journal of  
429 Hydrogen Energy, 37(19): 14265-14277.
- 430 Parkes, D., Evans, D.J., Williamson, P. and Williams, J.D.O., 2018. Estimating available salt volume for  
431 potential CAES development: A case study using the Northwich Halite of the Cheshire Basin.  
432 J. Energy Storage, 18: 50-61.
- 433 Russo, A. (1995). U.S. Patent No. 5,431,482. Washington, DC: U.S. Patent and Trademark Office.
- 434 Russo., A.J., 1983. User's manual for the salt solution mining code, SANSMIC.
- 435 Shi, X.L. et al., 2017. Development Prospect of Salt Cavern Gas Storage and New Research Progress  
436 of Salt Cavern Leaching in China, 51st U.S. Rock Mechanics/Geomechanics Symposium.  
437 American Rock Mechanics Association, San Francisco, California, USA, pp. 10.
- 438 Slizowski, J., Lankof, L., Urbanczyk, K. and Serbin, K., 2017a. Potential capacity of gas storage caverns  
439 in rock salt bedded deposits in Poland. Journal of Natural Gas Science and Engineering, 43:  
440 167-178.
- 441 Slizowski, J., Urbanczyk, K., Laciak, M., Lankof, L. and Serbin, K., 2017b. Effectiveness of natural gas  
442 and hydrogen storage in salt caverns. Przem. Chem., 96(5): 994-998.
- 443 Wang, S.X., Zhang, X.L., Yang, L.W., Zhou, Y. and Wang, J.J., 2016. Experimental study of compressed  
444 air energy storage system with thermal energy storage. Energy, 103: 182-191.
- 445 Wang, T.T. et al., 2013. A new shape design method of salt cavern used as underground gas storage.  
446 Appl. Energy, 104: 50-61.
- 447 Wang, T.T., Yang, C.H., Wang, H.M., Ding, S.L. and Daemen, J.J.K., 2018. Debrining prediction of a salt  
448 cavern used for compressed air energy storage. Energy, 147: 464-476.
- 449 WILKE, F., OBERMOLLER, M. and GREENHOVEN, H., 2011. Solution Mining with Two Boreholes for  
450 Gas Storage in Zuidwending, the Netherlands, Solution Mining Research Institute Spring  
451 Conference, pp. 2-5.
- 452 Xue, Z.Y., 1994. Manual for salt industry. China Light Industry Press, Beijing, China.
- 453 Yang, C.H. et al., 2015. Feasibility analysis of using abandoned salt caverns for large-scale  
454 underground energy storage in China. Appl. Energy, 137: 467-481.
- 455 Zhang, N. et al., 2017. Stability and availability evaluation of underground strategic petroleum  
456 reserve (SPR) caverns in bedded rock salt of Jintan, China. Energy, 134: 504-514.
- 457 Zheng, Y. et al., 2018. Small-spacing twin well natural solution and communication technology for  
458 solution mining of salt cavern underground gas storages. Natural Gas Industry, 38(3): 96-102.
- 459 Zhicheng, Z., Weiyao, Z., Wenwen, S. and Yujin, W., 2004. Mathematical model of chamber building  
460 with water solution for gas storages in salt beds. Natural Gas Industry, 24: 126-129.
- 461

## Highlights

For this article, we have summarized three highlights.

- 1) A 3D mathematical model based on Navier-Stokes equation of TWH salt cavern leaching construction for UGS was proposed for the first time.
- 2) The numerical calculation method of flow and mass transfer and the boundary movement was established.
- 3) A VC++ computer program for the TWH salt cavern was developed and was in good agreement with the experimental results.